Published in final edited form as:
J Neurosci Methods. 2008 July 15; 172(1): 137–141. doi:10.1016/j.jneumeth.2008.04.012.

An improved approach to detection of amplitude of low-frequency fluctuation (ALFF) for resting-state fMRI: Fractional ALFF

Qi-Hong Zou[a], **Chao-Zhe Zhu**[a], **Yihong Yang**[b], **Xi-Nian Zuo**[c], **Xiang-Yu Long**[a,c], **Qing-Jiu Cao**[d], **Yu-Feng Wang**[d], and **Yu-Feng Zang**[a,e,*]

[a]State Key Laboratory of Cognitive Neuroscience and Learning, Beijing Normal University, PR China

[b]Neuroimaging Research Branch, National Institute on Drug Abuse, National Institutes of Health, Baltimore, MD 21042, USA

[c]National Laboratory of Pattern Recognition, Institute of Automation, Chinese Academy of Sciences, PR China

[d]Institute of Mental Health, Peking University, Beijing, PR China

[e]Anding Hospital and Department of Psychiatry, Capital Medical University, Beijing, PR China

Abstract

Most of the resting-state functional magnetic resonance imaging (fMRI) studies demonstrated the correlations between spatially distinct brain areas from the perspective of functional connectivity or functional integration. The functional connectivity approaches do not directly provide information of the amplitude of brain activity of each brain region within a network. Alternatively, an index named amplitude of low-frequency fluctuation (ALFF) of the resting-state fMRI signal has been suggested to reflect the intensity of regional spontaneous brain activity. However, it has been indicated that the ALFF is also sensitive to the physiological noise. The current study proposed a fractional ALFF (fALFF) approach, i.e., the ratio of power spectrum of low-frequency (0.01–0.08 Hz) to that of the entire frequency range and this approach was tested in two groups of resting-state fMRI data. The results showed that the brain areas within the default mode network including posterior cingulate cortex, precuneus, medial prefrontal cortex and bilateral inferior parietal lobule had significantly higher fALFF than the other brain areas. This pattern was consistent with previous neuroimaging results. The non-specific signal components in the cistern areas in resting-state fMRI were significantly suppressed, indicating that the fALFF approach improved the sensitivity and specificity in detecting spontaneous brain activities. Its mechanism and sensitivity to abnormal brain activity should be evaluated in the future studies.

Keywords

Functional magnetic resonance imaging; Resting state; Amplitude of low-frequency fluctuation (ALFF); Spontaneous brain activity

[*]Corresponding author at: State Key Laboratory of Cognitive Neuroscience and Learning, Beijing Normal University, Beijing 100875, PR China. Tel.: +86 10 58801023; fax: +86 10 58801023. zangyf@263.net, zangyf@gmail.com (Y.-F. Zang).

1. Introduction

Recently, there has been increasing interest in using functional magnetic resonance imaging (fMRI) to investigate the ongoing neuronal processes at the “resting” state. Biswal and colleagues first reported that the spontaneous low-frequency (0.01–0.08 Hz) fluctuations (LFFs) in fMRI were highly synchronous between the right and left primary motor cortex at rest. The functional connectivity pattern of LFFs was quite similar to the activation pattern obtained from a bilateral finger-tapping task (Biswal et al., 1995), suggesting that LFFs might contain physiologically meaningful information. Combining electroneurophysiological recordings and fMRI, many studies have suggested that the LFFs of blood oxygena-level-dependent (BOLD) fMRI signals are closely related to the spontaneous neuronal activities (Goldman et al., 2002; Logothetis et al., 2001; Lu et al., 2007; Mantini et al., 2007). Numerous resting-state fMRI studies have revealed high synchronization of LFFs between the bilateral visual areas (Lowe et al., 1998), between the bilateral auditory areas (Cordes et al., 2000), within the language systems (Hampson et al., 2002) and within the default mode network (Greicius et al., 2003). Abnormal functional connectivity was found in a wide range of brain disorders including Alzheimer’s disease (Greicius et al., 2004; Wang et al., 2006), attention deficit hyperactivity disorder (Castellanos et al., 2008; Tian et al., 2006; Uddin et al., 2008), depression (Anand et al., 2005), schizophrenia (Jafri et al., 2008) and so on. Although functional connectivity analysis can provide us with more holistic information of a set of brain regions within a network, it does not reveal the BOLD signals change of the regional spontaneous activity. Moreover, abnormal connectivity among brain regions could not tell us precisely in which brain region the spontaneous activity is abnormal.

Detection of regional abnormalities is crucial to the clinical studies and even clinical applications. Resting-state positron emission tomography (PET) and electroencephalography (EEG) are two fundamental neuroimaging tools that are widely used in clinical practice. PET is used to evaluate the abnormality of regional brain metabolism and EEG can be used to reveal the changes of the power spectrum at some specific electrode positions. For the resting-state fMRI, such a robust index for detecting regional activity is lacking. Nevertheless, a few resting-state fMRI studies have investigated the regional brain activities. For example, it was reported that the root mean square (rms) of the LFFs in white matter was lower than that in gray matter by about 60% (Biswal et al., 1995; Li et al., 2000). Kiviniemi et al. (2000) used relative power of the peak over the noise fit to generate “resting activation” map in the visual cortex, and the results were similar to that obtained from correlation analysis. Using a discrete cosine basis set containing 120 regressors that spanned the frequency range of 0–0.1 Hz, Fransson (2005) found strong spontaneous fluctuation within the default mode network. Furthermore, Fransson (2006) indicated that the mean power spectral density of intrinsic LFFs in the default mode network was significantly decreased during a working memory task compared to rest. Based on the previous studies, Zang et al. (2007) developed an index, amplitude of LFFs (ALFF) in which the square root of power spectrum was integrated in a low-frequency range, for detecting the regional intensity of spontaneous fluctuations in BOLD signal. This index was subsequently used to differentiate two resting states, i.e., eyes open vs. eyes closed (Yang et al., 2007). Furthermore, ALFF has already been applied to patient studies including attention deficit hyperactivity disorder (Zang et al., 2007) and early Alzheimer’s disease (He et al., 2007).

Although ALFF seems to be a promising method for detecting regional signals change of spontaneous activity, an important issue remains unclear. Raichle et al. (2001) have demonstrated that the posterior cingulate cortex/precuneus (PCC/PCu), medial prefrontal cortex (MPFC) and bilateral inferior parietal lobule (IPL), which constitute the so-called default mode network, consistently showed significantly higher activity (i.e., oxygen

consumption and blood flow) than the global mean at rest. Similarly, Zang et al. (2007) performed a one-sample *t*-test and found that the PCC/PCu and MPFC showed significant higher ALFF than the global mean ALFF. However, some cistern areas also showed significant higher ALFF (Zang et al., 2007), probably due to higher physiological noise in these areas.

The aim of the current study is to examine resting-state fMRI signals in cisterns and cortical areas, and seek to improve the ALFF analysis method. We propose a fractional ALFF (fALFF) approach, in which the ratio of power spectrum of low-frequency (0.01–0.08 Hz) range to that of the entire frequency range was computed. We further test this improved approach on two-independent data sets.

2. Material and methods

2.1. Subjects

Subjects comprised of two groups: 24 boys and 16 adults (8 females), respectively. The data of the boy group was from the control group of a previous study (Cao et al., 2006) and the adult group data was also used in a previous study (Zang et al., 2004). All subjects were right-handed healthy volunteers with no history of head trauma, neurological or psychiatric disorders. Data from 2 boys and 2 adults were excluded from further analysis due to excessive head motion (see details in Section 2.3). Therefore, there were 22 boys (11.3–14.9 years, 13.3 ± 1.0 years) and 14 adults (7 females, 21–31 years, 24.7 ± 2.8 years) left. Before MRI scanning, written informed consents were obtained from all the adult subjects and the parents or guardians of all the boys. All the children agreed to participate in the study.

2.2. Imaging protocol

MRI data were acquired on a SIEMENS Trio 3T scanner in the Institute of Biophysics, Chinese Academy of Sciences. Subjects lay supine with the head snugly fixed by a belt and foam pads to minimize head motion. During resting-state fMRI scanning, subjects were instructed to close their eyes and keep still as much as possible, and not to think of anything systematically or fall asleep. The resting-state functional images for the boy group were acquired with the following parameters: TR = 2000 ms, TE = 30 ms, flip angle = 90°, in-plane resolution = 64 × 64, FOV = 220 mm × 220 mm, 30 axial slices, thickness/gap = 4.5/0 mm and 240 volumes (8 min). For the adult group, parameters were: TR = 2000 ms, TE = 30 ms, flip angle = 90°, in-plane resolution = 64 × 64, FOV = 220 mm × 220 mm, 32 axial slices, thickness/gap = 3.0/0.75 mm, 4 of the 16 adults having 208 volumes and the others having 240 volumes. For both groups, a 3D T1-weighted image was acquired covering the whole brain (176 sagittal slices for the boy group and 192 sagittal slices for the adult group). Other parameters were the same for both groups: TR = 1730 ms, TE = 3.93 ms, flip angle = 15°, in-plane resolution = 256 × 256, FOV = 240 mm × 240 mm and thickness/gap = 1.0/0 mm).

2.3. Data preprocessing

The first 8 volumes were discarded for MRI signal to reach a steady state, and for the subjects to get used to the scanner noise. For subjects who were scanned 240 volumes, the last 32 volumes were discarded in order that all subjects had the same length of time series in further processing. Part of the data preprocessing, including slice timing, head motion correction (a least squares approach and a 6-parameter spatial transformation) and spatial normalization to the Montreal Neurological Institute (MNI) template (resampling voxel size = 3 mm × 3 mm × 3 mm), were conducted using the Statistical Parametric Mapping (SPM5, http://www.fil.ion.ucl.ac.uk/spm) package. Subjects (2 boys and 2 adults) with head motion more than 3.0 mm of maximal translation (in any direction of *x*, *y* or *z*) or 1.0° of maximal

rotation throughout the course of scanning were excluded from further analysis. Further processing of the resting-state fMRI data was performed using AFNI (analysis of functional neuroimaging, http://afni.nimh.nih.gov) software (Cox, 1996).

2.4. ALFF analysis (the original approach)

After preprocessing in SPM, linear trend was removed. Then the fMRI data were temporally band-pass filtered ($0.01 < f < 0.08$ Hz) to reduce the very low-frequency drift and high-frequency respiratory and cardiac noise (Biswal et al., 1995; Lowe et al., 1998). ALFF analysis (Yang et al., 2007; Zang et al., 2007) was performed using the AFNI software. The time series for each voxel was transformed to the frequency domain and the power spectrum was then obtained. Since the power of a given frequency is proportional to the square of the amplitude of this frequency component, the square root was calculated at each frequency of the power spectrum and the averaged square root was obtained across 0.01–0.08 Hz at each voxel. This averaged square root was taken as the ALFF (Zang et al., 2007). In our previous work (Zang et al., 2007), the ALFF of each voxel was divided by the individual global mean of ALFF within a brain-mask, which was obtained by removing the tissues outside the brain using software MRIcro (by Chris Rorden, http://www.psychology.nottingham.ac.uk/staff/cr1/mricro.html. See original Ref. of Smith, 2002). This standardization procedure is the same as that used in PET studies (Raichle et al., 2001). In the current work, the individual data was transformed to *Z* score (i.e., minus the global mean value and then divided by the standard deviation) other than simply being divided by the global mean. Spatial smoothing was conducted on the *Z* maps with an isotropic Gaussian kernel of 8 mm of full-width at half-maximum. The *Z* maps were transformed to the Talairach and Tournoux coordinates (Talairach and Tournoux, 1988) and one-sided one-sample *t*-test was performed on the *Z* maps within the boy group and the adult group, respectively.

2.5. fALFF analysis (the improved approach)

As shown in Fig. 1a and c, although the original ALFF approach revealed significant higher ALFF in the PCC, PCu and MPFC, it also showed significant higher ALFF in non-specific areas such as cisterns, ventricles and/or vicinity of large blood vessels. This result was consistent to our previous results (Zang et al., 2007). The time series (without filtering) from a typical voxel in the suprasellar cistern (Talairach coordinates (−1, −2, −18)) of an individual demonstrated higher fluctuations than that of a voxel from PCC (Talairach coordinates (−4, −56, 25)) (Fig. 2a). The corresponding power spectrum of this typical voxel in the suprasellar cistern showed that its power at almost every frequency was higher than that in PCC (Fig. 2b). To improve the original ALFF approach, a ratio of the power of each frequency at the low-frequency range (0.01–0.08 Hz) to that of the entire frequency range (0–0.25 Hz), i.e., fractional ALFF (fALFF) was used (Fig. 2c). The procedure of data analysis of fALFF was similar to Section 2.4 mentioned above. After the linear trend was removed, the time series for each voxel were transformed to a frequency domain without band-pass filtering. The square root was calculated at each frequency of the power spectrum. The sum of amplitude across 0.01–0.08 Hz was divided by that across the entire frequency range, i.e., 0–0.25 Hz. Further procedures were the same as in Section 2.4.

To further compare the ALFF and fALFF, a few typical voxels from some areas were selected, including the lateral ventricle (5, −6, 21), suprasellar cistern (−1, −2, −18), ambient cistern (16, −14, −22), Sylvian fissure (−41, 11, −6), MPFC (−2, 38, 17) and PCC (−4, −56, 25) in the boy group and adult group. The *Z* scores (standardized ALFF and fALFF value) of these typical voxels were presented.

3. Results and discussion

As predicted, the one-sample *t*-tests of the original ALFF analysis show significant higher ALFF in the PCC, PCu and MPFC (Fig. 1a and c). These results are consistent with previous resting-state PET studies (Raichle et al., 2001) and resting-state fMRI studies (Fransson, 2005; He et al., 2004), indicating that the higher ALFF within these areas may reflect higher spontaneous neuronal activity during resting but awake state. However, significantly higher ALFF can also been seen in the suprasellar cistern, ambient cistern, the ventricles and/or vicinity of large blood vessels, such as the carotid artery, basilar artery and sagittal sinus (Fig. 1a and c). This suggests that the original ALFF approach may be sensitive to signal fluctuations contributed from physiological noise irrelevant to brain activity.

The individual time series (without temporal filtering) and power spectrum of typical voxels from the suprasellar cistern and PCC demonstrate the effect of physiological noise and improvement by the power ratio analysis using fALFF (Fig. 2). The amplitude of fluctuations in the suprasellar cistern is much higher than that in the PCC (Fig. 2a). The power spectrum of the time series in the suprasellar cistern is higher at almost every frequency than that of the PCC, especially at the higher frequency range (>0.08 Hz, see Fig. 2b). The entire frequency range may be affected by physiological noise induced by cardiac and respiratory pulsations (Birn et al., 2006; Hu et al., 1995; Lund et al., 2006; Shmueli et al., 2007; Wise et al., 2004). After the power spectrum fractionalizing was performed, the power of the lower frequency range in the suprasellar cistern becomes lower than that in the PCC (Fig. 2c), while the power of high-frequency range is still higher for the voxel in suprasellar cistern. These results suggest that resting-state fMRI signals in the cortical and cistern areas may have distinct characteristics in terms of their power distribution at different frequency ranges. The distinct frequency properties may be utilized to distinguish noise from signal associated with the LFFs, although the underlying mechanism remains to be further revealed.

The *t*-test results of fALFF analysis for the both groups show that the brain areas within the default mode network have significantly higher fALFF than the rest of the brain (Fig. 1b and d), well consistent with the previous results (He et al., 2004; Raichle et al., 2001). The physiological noise in the cisterns and ventricles that was found by the original ALFF approach was successfully suppressed with the fALFF approach (Fig. 1b and d). The bilateral IPLs have been consistently reported to be important components in the default mode network (Greicius et al., 2003; Gusnard and Raichle, 2001; He et al., 2004; Raichle et al., 2001; Zang et al., 2004), and these areas are robustly detected using fALFF analysis (Fig. 1a vs. Fig. 1b, Fig. 1c vs. Fig. 1d). However, as shown in Fig. 1b and d, some brain regions, such as the temporal–parietal regions and the precentral gyrus, which are not part of the default mode network (Raichle et al., 2001), also showed significant higher fALFF. This might be a potential limitation for the current fALFF analysis. From a methodological point of view, both PET and the current fALFF are for measurement of local brain activity. However, the relationship between cerebral metabolism or blood flow and the present fALFF is unclear. The mechanism of the fALFF method needs to be further studied.

Fig. 3 illustrates the *Z* scores (mean ± S.D.) of the ALFF and fALFF analyses in the selected brain regions from the boy group (Fig. 3a) and adult group (Fig. 3b). The *Z* scores of fALFF reduce prominently in the ventricle and cistern areas, while increasing sizably in the PCC and MPFC, comparing to that of ALFF. Detailed comparison was shown in the following when taking the boy group as an example. In the suprasellar cistern, the *Z* scores of ALFF are significantly higher than the global mean values ($t = 11.44$), while the *Z* scores of fALFF in the same brain region are changed to be significantly lower than the global mean ($t = -8.09$), indicated that the physiological noise can be effectively suppressed by the fALFF

approach. The PCC is one important node of the default mode network (Raichle et al., 2001), with higher ALFF (t = 8.66), and the fALFF values of the PCC are more significant (t = 14.89). The results demonstrate that the fALFF method is more sensitive to detect the neuronal activity. Thus the fALFF approach selectively suppresses artifacts from non-specific brain areas, while enhances signals from cortical regions associated with brain activity, making use of the distinct characteristics of their signals in the frequency domain.

In summary, the results of current study demonstrated that the fractional ALFF approach, i.e., the ratio of power spectrum of low frequency (0.01–0.08 Hz) to that of the entire frequency range (0–0.25 Hz, with TR = 2 s), may effectively suppress non-specific signal components in the resting-state fMRI, and therefore would significantly improve the sensitivity and specificity in detecting regional spontaneous brain activity. Its mechanism, e.g., the relationship between fALFF and cerebral blood flow or oxygen metabolism needs to be evaluated in the future studies. Moreover, its sensitivity to brain disorders should be explored in more application studies.

Acknowledgments

This work was supported by Natural Science Foundation of China (30470575, 30530290, 30621130074 and 30770594) and by National Key Basic Research and Development Program (973) (2003CB716101).

References

Anand A, Li Y, Wang Y, Wu J, Gao S, Bukhari L, et al. Activity and connectivity of brain mood regulating circuit in depression: a functional magnetic resonance study. Biol Psychiatry. 2005; 57:1079–88. [PubMed: 15866546]

Birn RM, Diamond JB, Smith MA, Bandettini PA. Separating respiratory-variation-related fluctuations from neuronal-activity-related fluctuations in fMRI. NeuroImage. 2006; 31:1536–48. [PubMed: 16632379]

Biswal B, Yetkin FZ, Haughton VM, Hyde JS. Functional connectivity in the motor cortex of resting human brain using echo-planar MRI. Magn Reson Med. 1995; 34:537–41. [PubMed: 8524021]

Cao Q, Zang Y, Sun L, Sui M, Long X, Zou Q, et al. Abnormal neural activity in children with attention deficit hyperactivity disorder: a resting-state functional magnetic resonance imaging study. Neuroreport. 2006; 17:1033–6. [PubMed: 16791098]

Castellanos FX, Margulies DS, Kelly C, Uddin LQ, Ghaffari M, Kirsch A, et al. Cingulate–precuneus interactions: a new locus of dysfunction in adult attention-deficit/hyperactivity disorder. Biol Psychiatry. 2008; 63:332–7. [PubMed: 17888409]

Cordes D, Haughton VM, Arfanakis K, Wendt GJ, Turski PA, Moritz CH, et al. Mapping functionally related regions of brain with functional connectivity MR imaging. AJNR. 2000; 21:1636–44. [PubMed: 11039342]

Cox RW. AFNI: software for analysis and visualization of functional magnetic resonance neuroimages. Comput Biomed Res. 1996; 29:162–73. [PubMed: 8812068]

Fransson P. Spontaneous low-frequency BOLD signal fluctuations: an fMRI investigation of the resting-state default mode of brain function hypothesis. Hum Brain Mapp. 2005; 26:15–29. [PubMed: 15852468]

Fransson P. How default is the default mode of brain function? Further evidence from intrinsic BOLD signal fluctuations. Neuropsychologia. 2006; 44:2836–45. [PubMed: 16879844]

Goldman RI, Stern JM, Engel J Jr, Cohen MS. Simultaneous EEG and fMRI of the alpha rhythm. Neuroreport. 2002; 13:2487–92. [PubMed: 12499854]

Greicius MD, Krasnow B, Reiss AL, Menon V. Functional connectivity in the resting brain: a network analysis of the default mode hypothesis. Proc Natl Acad Sci USA. 2003; 100:253–8. [PubMed: 12506194]

Greicius MD, Srivastava G, Reiss AL, Menon V. Default-mode network activity distinguishes Alzheimer's disease from healthy aging: evidence from functional MRI. Proc Natl Acad Sci USA. 2004; 101:4637–42. [PubMed: 15070770]

Gusnard DA, Raichle ME. Searching for a baseline: functional imaging and the resting human brain. Nat Rev Neurosci. 2001; 2:685–94. [PubMed: 11584306]

Hampson M, Peterson BS, Skudlarski P, Gatenby JC, Gore JC. Detection of functional connectivity using temporal correlations in MR images. Hum Brain Mapp. 2002; 15:247–62. [PubMed: 11835612]

He Y, Wang L, Zang Y, Tian L, Zhang X, Li K, et al. Regional coherence changes in the early stages of Alzheimer's disease: a combined structural and resting-state functional MRI study. NeuroImage. 2007; 35:488–500. [PubMed: 17254803]

He Y, Zang YF, Jiang TZ, Liang M, Gong GL. Detecting functional connectivity of the cerebellum using low frequency fluctuations (LFFs). Medical image computing and computer-assisted intervention. Lect Notes Comput Sci. 2004; 3217:907–15.

Hu X, Le TH, Parrish T, Erhard P. Retrospective estimation and correction of physiological fluctuation in functional MRI. Magn Reson Med. 1995; 34:201–12. [PubMed: 7476079]

Jafri MJ, Pearlson GD, Stevens M, Calhoun VD. A method for functional network connectivity among spatially independent resting-state components in schizophrenia. NeuroImage. 2008; 39(4):1666–81. [PubMed: 18082428]

Kiviniemi V, Jauhiainen J, Tervonen O, Paakko E, Oikarinen J, Vainionpaa V, et al. Slow vasomotor fluctuation in fMRI of anesthetized child brain. Magn Reson Med. 2000; 44:373–8. [PubMed: 10975887]

Li SJ, Biswal B, Li Z, Risinger R, Rainey C, Cho JK, et al. Cocaine administration decreases functional connectivity in human primary visual and motor cortex as detected by functional MRI. Magn Reson Med. 2000; 43:45–51. [PubMed: 10642730]

Logothetis NK, Pauls J, Augath M, Trinath T, Oeltermann A. Neurophysiological investigation of the basis of the fMRI signal. Nature. 2001; 412:150–7. [PubMed: 11449264]

Lowe MJ, Mock BJ, Sorenson JA. Functional connectivity in single and multislice echo-planar imaging using resting-state fluctuations. NeuroImage. 1998; 7:119–32. [PubMed: 9558644]

Lu H, Zuo Y, Gu H, Waltz JA, Zhan W, Scholl CA, et al. Synchronized delta oscillations correlate with the resting-state functional MRI signal. Proc Natl Acad Sci USA. 2007; 104:18265–9. [PubMed: 17991778]

Lund TE, Madsen KH, Sidaros K, Luo WL, Nichols TE. Non-white noise in fMRI: does modelling have an impact? NeuroImage. 2006; 29:54–66. [PubMed: 16099175]

Mantini D, Perrucci MG, Del Gratta C, Romani GL, Corbetta M. Electrophysiological signatures of resting state networks in the human brain. Proc Natl Acad Sci USA. 2007; 104:13170–5. [PubMed: 17670949]

Raichle ME, MacLeod AM, Snyder AZ, Powers WJ, Gusnard DA, Shulman GL. A default mode of brain function. Proc Natl Acad Sci USA. 2001; 98:676–82. [PubMed: 11209064]

Shmueli K, Gelderen PV, de Zwart JA, Horovitz SG, Fukunaga M, Jansma JM, et al. Low-frequency fluctuations in the cardiac rate as a source of variance in the resting-state fMRI BOLD signal. NeuroImage. 2007; 38:306–20. [PubMed: 17869543]

Smith SM. Fast robust automated brain extraction. Hum Brain Mapp. 2002; 17:143–55. [PubMed: 12391568]

Talairach, J.; Tournoux, PA. Coplanar stereotactic atlas of the human brain. Thieme; Stuttgart: 1988.

Tian L, Jiang T, Wang Y, Zang Y, He Y, Liang M, et al. Altered resting-state functional connectivity patterns of anterior cingulate cortex in adolescents with attention deficit hyperactivity disorder. Neurosci Lett. 2006; 400:39–43. [PubMed: 16510242]

Uddin LQ, Kelly AM, Biswal BB, Margulies DS, Shehzad Z, Shaw D, et al. Network homogeneity reveals decreased integrity of default-mode network in ADHD. J Neurosci Methods. 2008; 169:249–54. [PubMed: 18190970]

Wang L, Zang Y, He Y, Liang M, Zhang X, Tian L, et al. Changes in hippocampal connectivity in the early stages of Alzheimer's disease: evidence from resting state fMRI. NeuroImage. 2006; 31:496–504. [PubMed: 16473024]

Wise RG, Ide K, Poulin MJ, Tracey I. Resting fluctuations in arterial carbon dioxide induce significant low frequency variations in BOLD signal. NeuroImage. 2004; 21:1652–64. [PubMed: 15050588]

Yang H, Long XY, Yang YH, Yan H, Zhu CZ, Zhou XP, et al. Amplitude of low frequency fluctuation within visual areas revealed by resting-state functional MRI. NeuroImage. 2007; 36:144–52. [PubMed: 17434757]

Zang Y, Jiang T, Lu Y, He Y, Tian L. Regional homogeneity approach to fMRI data analysis. NeuroImage. 2004; 22:394–400. [PubMed: 15110032]

Zang YF, He Y, Zhu CZ, Cao QJ, Sui MQ, Liang M, et al. Altered baseline brain activity in children with ADHD revealed by resting-state functional MRI. Brain Dev. 2007; 29:83–91. [PubMed: 16919409]

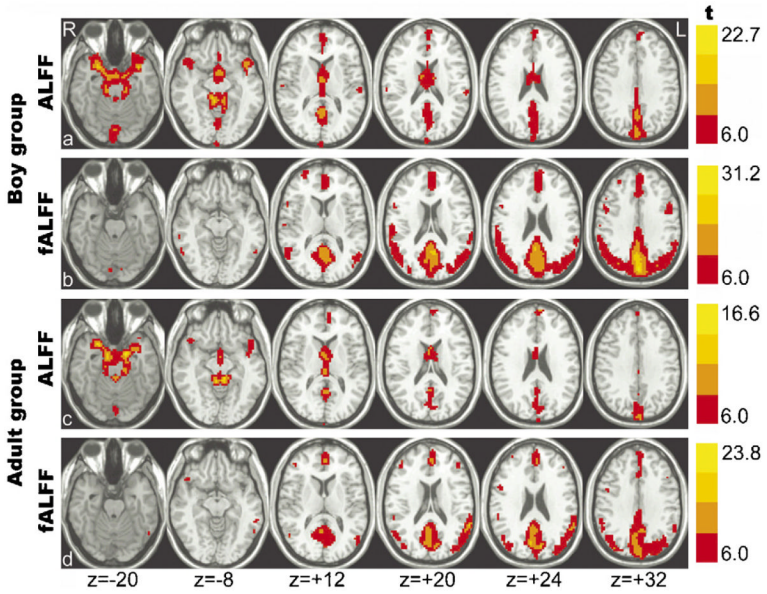

Fig. 1.

The results of one-sided one-sample *t*-tests of the original ALFF (a and c) and fALFF (b and d) approach, in the boy group (a and b) ($n = 22$, $t > 6.0$, $p < 6.0 \times 10^{-6}$, uncorrected) and adult group (c and d) ($n = 14$, $t > 6.0$, $p < 4.5 \times 10^{-5}$, uncorrected). The *t* maps were overlaid on the 3D images in the MRIcro software.

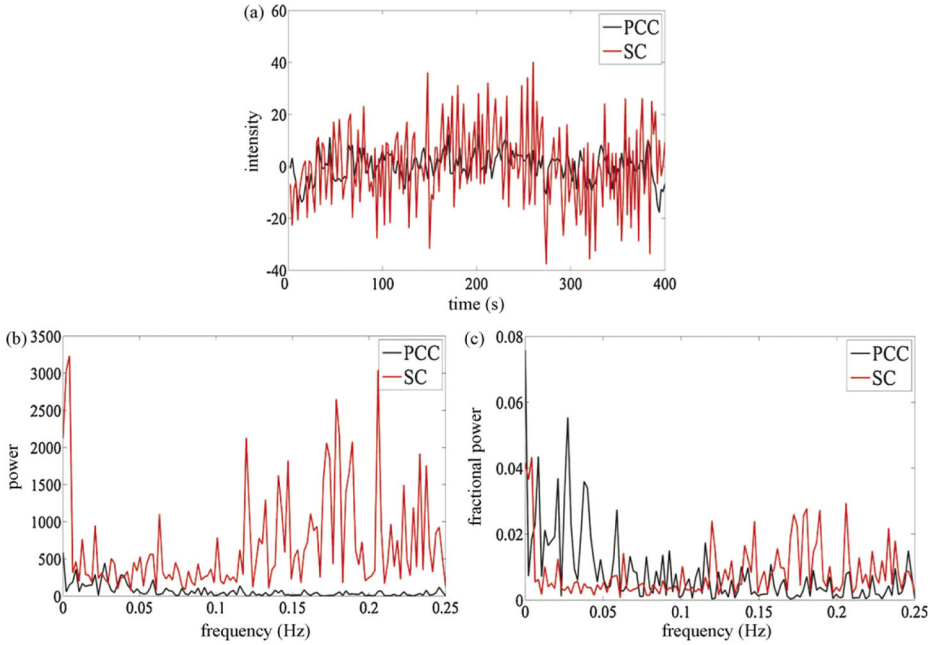

Fig. 2.

Illustration of the improvement of ALFF approach. (a) The time series (without filtering) from a typical voxel in the suprasellar cistern (SC) (−1, −2, −18) and the posterior cingulate cortex (PCC) (−4, −56, 25) of an individual. (b) The power in the SC is higher than that in PCC at almost every frequency. (c) The ratio of the power at each frequency to the integrate power of the entire frequency range indicates that the power in the low-frequency range (0.01–0.08 Hz) is significantly suppressed in the SC.

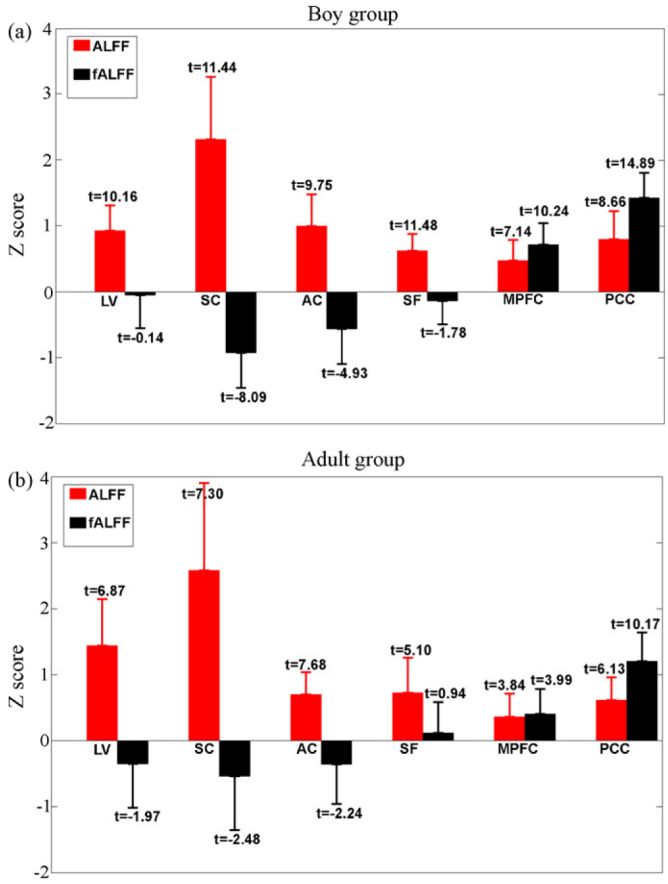

Fig. 3.

The *Z* scores (standardized ALFF and fALFF values) and the corresponding *t* values (one-sample *t*-test) of a few typical voxels selected from some areas in the boy group (a) and adult group (b). LV, lateral ventricle (5, −6, 21); SC, suprasellar cistern (−1, −2, −18); AC, ambient cistern (16, −14, −22); SF, Sylvian fissure (−41, 11, −6); MPFC, medial prefrontal cortex (−2, 38, 17); PCC, posterior cingulate cortex (−4, −56, 25).